J|A|C|S COMMUNICATIONS

Published on Web 01/07/2010

Chemically Programmed Ultrahigh Density Two-Dimensional Semiconductor Superlattice Array

Narayan Pradhan,[†,§] Somobrata Acharya,*[,‡,§] Katsuhiko Ariga,[‡] Niladri S. Karan,[§] D. D. Sarma,[§,||] Yoshiki Wada,[‡] Shlomo Efrima,[†,#] and Yuval Golan[⊥]

Department of Chemistry, Ben-Gurion University of the Negev, Beer-Sheva, Israel 84105, World Premier International (WPI) Research Center for Materials Nanoarchitectonics (MANA), National Institute for Materials Science (NIMS), 1-1 Namiki, Tsukuba, Ibaraki 305-0044, Japan, Centre for Advanced Materials, Indian Association for the Cultivation of Science, Kolkata 700032, India, Solid State and Structural Chemistry Unit and Centre for Condensed Matter Theory, Indian Institute of Science, Bangalore 560012, India, and Department of Materials Engineering and Ilse Katz Institute for Meso and Nanoscale Science and Technology, Ben-Gurion University of the Negev, Beer-Sheva, Israel 84105

Received October 24, 2009; E-mail: camsa2@iacs.res.in

A superlattice is a periodic array of interactive quantum wells formed by materials with different band gaps.[1] The diverse functionality arises from the energy gap variations at the interface that control the carrier flow, leading to numerous devices with many potential applications.[2] The conventional superlattice-fabrication strategies based on vapor−liquid−solid growth (VLS) or molecular beam epitaxy (MBE) techniques are limited by their application limit, while a direct synthetic route could provide an alternative means of creating high-density superlattices. However, designing an ultrahigh density linear superlattice array consisting of periodic blocks of different-band-gap semiconductors in the strong confinement regime via a direct synthetic route remains an unachieved challenge in nanotechnology. Partial ion exchange demonstrates such capabilities in producing metal−semiconductor superlattice structures,[3] though this method is deficient in producing a large area of alternating blocks with enhanced repeat density, as required for ultrahigh density junction-based applications. Here we report a general synthesis route for the formulation of a large-area ultrahigh density superlattice array that involves adjoining multiple units of higher-band-gap ZnS rods by lower-band-gap prolate CdS particles at the tips. A single one-dimensional (1D) wire is 300−500 nm long and consists of periodic quantum wells with barrier widths of 5 nm provided by the 1.2 nm wide ZnS rods and well widths of 1−2 nm provided by the CdS particles, defining the superlattice structure. The superlattice wires are self-assembled into two-dimensional (2D) supercrystalline arrays over an area of 2.5 μm^2 with an ultrahigh pitch density of 3.5 nm between adjacent nanowires. The synthesis route allows tailoring of ultranarrow laserlike emissions (fwhm $\approx$ 125 meV) originating from strong interwell energy dispersion along with control of the width, pitch, and registry of the superlattice assembly. Such an exceptional high-density superlattice array is of fundamental scientific importance because of its physical scale below the de Broglie wavelength and could form the basis of ultrahigh density memories in addition to offering opportunities for technological advancement in conventional heterojunction-based device applications.

We first formed 2D supercrystalline ZnS rods by decomposition of zinc ethylxanthate[4a,b] and then decomposed cadmium hexadecylxanthate under the same reaction conditions to form a 1D $(-ZnS-CdS-ZnS-)_n$ superlattice system [see the Supporting Information (SI)]. The width of a single superlattice wire varied periodically between 1.2 and 2 nm with lengths of 300−500 nm, defining a high aspect ratio (Figure 1a). The superlattice wires were self-assembled into a 2D supercrystalline structure over an area of 2.5 μm^2 by simple drop-casting from a suspension while maintaining tight side-by-side registry induced by the capping agents. The pitch evaluated using statistical profile analysis (Figure 1a inset) revealed a distance of 3.5 ± 0.05 nm between adjacent nanowires.

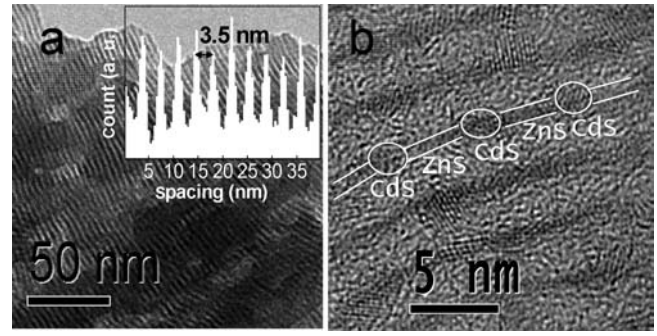

Figure 1. (a) TEM image of a 2D supercrystalline parallel assembly of $(-ZnS-CdS-ZnS-)_n$ superlattice wires. Inset: statistical distribution of superlattices demonstrating an ultrahigh pitch density of 3.5 nm. (b) HRTEM image of a 2D supercrystalline parallel assembly of $(-ZnS-CdS-ZnS-)_n$ superlattice wires.

The high-resolution transmission electron microscopy (HRTEM) image (Figure 1b; also see the SI) clearly shows two distinct periodic regions: one has a diameter of ∼1.2 nm and a length of 5 nm, which are the same as for the initial ZnS rods (see the SI),[4a] and the other is a thicker anchoring region at the tips of the rods, originating from the less than 2 nm wide prolate CdS particles. The narrower 1.2 nm linear regions show well-resolved lattice planes with an interplanar spacing of 0.32 ± 0.005 nm, corresponding to $(00.2)_{ZnS}$ wurtzite nanorods, and the bulges show interplanar spacings of 0.35 ± 0.007 nm that are consistent mainly with the $(10.0)_{CdS}$ d spacing of the CdS wurtzite structure.[4a,c] However, spacings of 0.33 ± 0.05 nm corresponding to $(00.2)_{CdS}$ wurtzite planes forming a continuous lattice with the $(00.2)_{ZnS}$ planes were also observed (see the SI). The powder X-ray diffraction pattern from the superlattice wires corresponds to these wurtzite phases, in agreement with the HRTEM images (see the SI).

We applied various techniques such as energy-dispersive X-ray spectroscopy (EDS), nanoprobe electron energy-loss spectroscopy (EELS), *Z*-contrast imaging, and selected-area electron diffraction (SAED) to structurally probe the constituent blocks within the

[†] Department of Chemistry; Ben-Gurion University of the Negev.
[§] Indian Association for the Cultivation of Science.
[‡] National Institute for Materials Science.
[||] Indian Institute of Science.
[⊥] Department of Materials Engineering and Ilse Katz Institute for Meso and Nanoscale Science and Technology, Ben-Gurion University of the Negev.
[#] Deceased.

 10.1021/ja908868b

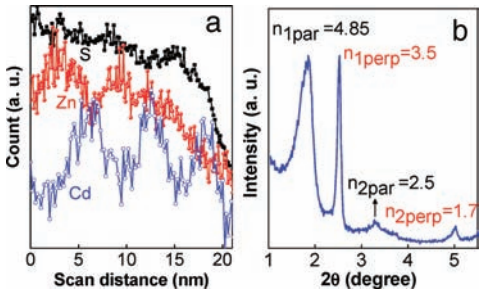

Figure 2. (a) EELS line scan profile along a superlattice wire showing the composition variation at each 5 nm repeat distance with Zn (red), Cd (blue), and S (black) traces. (b) SAXS data for superlattice wires in a toluene suspension. The orders of the diffraction peaks parallel (par) and perpendicular (perp) to the wire directions are indicated.

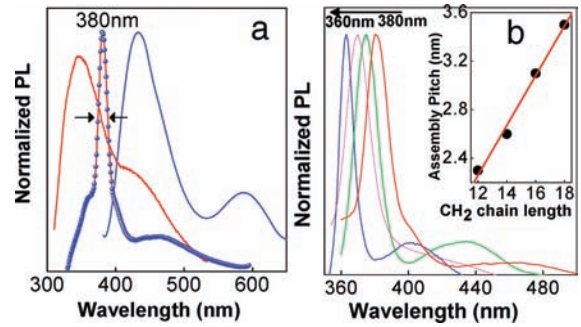

Figure 3. (a) PL spectra (excitation 300 nm) of 1.2 nm wide ZnS rods (red curve), 1.7 nm wide CdS rods (blue curve) and $(-ZnS-CdS-ZnS-)_n$ superlattices (red line with blue dots) suspended in toluene. (b) Tunability of the narrow intense band by using octadecylamine (red curve), hexadecylamine (green curve), tetradecylamine (magenta curve), and dodecylamine (blue curve). Inset: tunability of the assembly pitch by using different capping agents, offering control in the subnanometer regime.

superlattice (see the SI). The local atomic composition variation within the superlattice wires revealed by the EELS line scan shows traces of S throughout, with periodic ~5 nm regions of Zn and periodic traces of Cd localized at a distance 5 nm apart (Figure 2a; also see the SI). The length scale reasonably agrees with the superlattice structure model consisting of ~5 nm regions of ZnS and 1−2 nm regions of CdS. The small-angle X-ray scattering (SAXS) data in the diluted sample (Figure 2b) show a first peak at $2\theta = 1.84°$, corresponding to a distance of 4.85 nm, which matches well with the periodicity expected from the $(-ZnS-CdS-ZnS-)_n$ superlattice wires in view of the ~5 nm repeat lengths of the ZnS units within the superlattice wires. The sharp, high-intensity peak appearing at $2\theta = 2.52°$ corresponds well with the 3.5 nm center-to-center pitch between the wires observed by TEM. Since the parallel superlattice wire assembly is composed of alternating ZnS and CdS blocks, both the longitudinal and lateral periodicities are excellently reflected in the SAXS measurement over a long range.

The key parameters in designing the $(-ZnS-CdS-ZnS-)_n$ superlattice system are the 2D supercrystalline nature of wurtzite ZnS rods, which are prone to coalesce into longer wires; the use of an appropriate amount of cadmium xanthate precursor; and tuning of the reaction conditions (see the SI). The optical absorption spectra of the $(-ZnS-CdS-ZnS-)_n$ superlattice in toluene show well-resolved electronic transitions originating from the individual segments (see the SI). The photoluminescence (PL) spectra strongly support the linear superlattice formation by ZnS rods and CdS prolate particles (Figure 3a). The emission originating from the band edge of the 1.2 nm wide ZnS rods appears at 355 nm, and the visible emission registered at ~430 nm is similar to the excitonic emission shown by 1.7 nm reference CdS nanorods.[4c] Remarkably, the superlattices exhibit an unusual ultranarrow laserlike robust PL band at higher energy (380 nm; 3.27 eV) with a fwhm of 125 meV. We assign the emission as stemming from ultrasmall CdS regions interposed between the 5 nm long ZnS rods with preferential $(002)_{CdSZnS}$ lattice matching within the superlattice. Notably, both crystallographic phases are wurtzite, implying a preferential alignment with one another in which the dipole orientation of the individual segments is along the length of the wires, a condition favorable for exchange coupling.[5] The small barrier width of 5 nm in the superlattice probably allows coupling of the 1−2 nm wells, resulting in miniband formation.[6] The well widths of 1−2 nm are sufficiently smaller than the electronic mean free path. Thus, strong energy dispersion is expected, allocating a series of narrow allowed and forbidden bands associated with the minibands, which might cause enhanced transition energies within the wells that generate the observed ultranarrow intense emission. Importantly, the ultranarrow fluorescence can be tuned over a range of 20 nm by selectively changing the surfactant (Figure 3b). The confined space for CdS particles provided by ZnS rods at their tips can be controlled by the surfactant chain length, which changes the entrapped CdS size and allows the well widths to be varied with different confinement energies. Simultaneously, the side-by-side distance between the superlattice wires can also be tuned to control the pitch of the superstructured assembly (Figure 3b inset) by using surfactants with different chain lengths.

Assembling superlattice nanowires into highly ordered arrays over a large area with predetermined spacing and tight end-to-end registry has remained challenging. Our method is flexible, since the assembly pitch can be well-controlled in the subnanometer regime via the desired synthesis route along with a tunable PL energy. Semiconductor periodic junctions at a separation of 5 nm repeat unit imply an ultrahigh junction density on the order of petabits (10^{15}) per square centimeter, which could be used for memory storage devices upon proper addressing and also could provide the possibility of fabricating more sophisticated heterostructure-based components for optoelectronics and nanoelectronics.

Acknowledgment. Financial support from the World Premier International Research Center (WPI) Initiative on Materials Nanoarchitectonics, MEXT, Japan, the Centre for Nanotechnology for Photovoltaics and Sensor Devices, DST, Government of India (Grant SR/S5/NM-47/2005), and the U.S.−Israel Binational Science Foundation (Grant 2006032) is gratefully acknowledged. JEOL (Tokyo, Japan) and A. B. Panda are gratefully acknowledged for scientific support. N.P. acknowledges an LNJ Bhilwara Research Fellowship.

Supporting Information Available: Synthesis routes, TEM images of ZnS and CdS rods, HRTEM images of superlattice structure, structural characterizations using various techniques, UV−vis absorption spectra, and CdS particle size calculations. This material is available free of charge via the Internet at http://pubs.acs.org.

References

(1) (a) Esaki, L.; Tsu, R. *IBM J. Res. Dev.* **1970**, *14*, 6. (b) Kroemer, H. *Jpn. J. Appl. Phys.* **1981**, *20*, 9.
(2) (a) Gudiksen, M. S.; Lauhon, L. J.; Wang, J.; Smith, D. C.; Lieber, C. M. *Nature* **2002**, *415*, 617. (b) Kroemer, H. *Proc. IEEE* **1982**, *70*, 13. (c) Heath, J. R. *Acc. Chem. Res.* **2008**, *41*, 1609. (d) Milliron, D. J.; Hughes, S. M.; Chi, Y.; Manna, L.; Li, J.; Wang, L.-W.; Alivisatos, A. P. *Nature* **2004**, *430*, 190. (e) Halpert, J. E.; Porter, V. J.; Zimmer, J. P.; Bawendi, M. G. *J. Am. Chem. Soc.* **2006**, *128*, 12590.
(3) Robinson, R. D.; Sadtler, B.; Demchenko, D. O.; Erdonmez, C. K.; Wang, L.-W.; Alivisatos, A. P. *Science* **2007**, *317*, 355.
(4) (a) Pradhan, N.; Efrima, S. *J. Phys. Chem. B* **2004**, *108*, 11964. (b) Acharya, S.; Efrima, S. *J. Am. Chem. Soc.* **2005**, *127*, 3486. (c) Acharya, S.; Patla, I.; Kost, J.; Efrima, S.; Golan, Y. *J. Am. Chem. Soc.* **2006**, *128*, 9294.
(5) Collier, C. P.; Vossmeyer, T.; Heath, J. R. *Annu. Rev. Phys. Chem.* **1998**, *49*, 371.
(6) (a) Nozik, A. J. *Annu. Rev. Phys. Chem.* **2001**, *52*, 193. (b) Peterson, M. W.; Turner, J. A.; Parsons, C. A.; Nozik, A. J.; Arent, D. J.; Van Hoof, C.; Borghs, G.; Houdré, R.; Morkoç, H. *Appl. Phys. Lett.* **1988**, *53*, 2666.

JA908868B